

Site Preferences of Fluoride Guest Ions in the Calcium Silicate Phases of Portland Cement from $^{29}\text{Si}\{^{19}\text{F}\}$ CP-REDOR NMR Spectroscopy

Thuan T. Tran,[†] Duncan Herfort,[‡] Hans J. Jakobsen,[†] and Jørgen Skibsted^{*,†}

Instrument Centre for Solid-State NMR Spectroscopy and Interdisciplinary Nanoscience Center, Department of Chemistry, Aarhus University, DK-8000 Aarhus C, Denmark, and Aalborg Portland A/S, DK-9100 Aalborg, Denmark

Received June 25, 2009; E-mail: jskib@chem.au.dk

The reduction of CO₂ emission associated with cement production represents probably the most important and urgent challenge for the cement industry. The industry accounts for 5% of the global anthropogenic CO₂ emissions and must increase today's cement production by 2- to 3-fold to meet global demand by 2050.^{1,2} Roughly 40% of the CO₂ comes from the fuel used to heat the cement kilns while 60% originates from the decarbonation of limestone (CaCO₃) required to form the main cement phases alite (Ca₃SiO₅) and belite (Ca₂SiO₄). Common routes to reduce the CO₂ emissions include the partial replacement of Portland cement by supplementary cementitious materials (e.g., fly ashes from coal burning, slag from pig iron production, silica fume from the production of ferrosilicon) or the use of biofuels instead of coal in the cement kilns. Another approach for reducing emissions is to reduce fuel consumption either kinetically by improved homogenization of the raw materials etc. or thermodynamically by reducing the temperature at which the high temperature silicates form, particularly alite. This can be accomplished by fluoride mineralization which is the subject of this work, where a small amount of fluoride (e.g., CaF₂) added to the raw mix has a profound impact on the formation of alite.^{3–6} Fluoride ions are incorporated in alite by substitution for oxygen, resulting in an increased entropy of mixing which lowers the so-called burning-zone temperature in the cement kiln by up to 200 °C. The substitution is primarily charge-balanced by other guest ions (e.g., Al³⁺ for Si⁴⁺ substitution).⁴ The optimum fluorine content in terms of performance of the cement in the final application is ~0.2 wt % F for most Portland cements.⁵

Optimization of the entropy of mixing by fluoride mineralization, of course, depends on the types of oxygen sites accessible for F[–] substitution. In this work we locate these oxygen sites in the calcium silicate phases of a white Portland cement by double-resonance $^{29}\text{Si}\{^{19}\text{F}\}$ MAS NMR experiments which depend on ^{29}Si – ^{19}F dipolar interactions. Similar $^{29}\text{Si}\{^{19}\text{F}\}$ NMR techniques have earlier been used to locate the F[–] ion in fluoride silicalite (a MFI zeolite) from these NMR experiments alone.⁷ However, the low NMR sensitivity associated with the low fluorine content in the cements (0.04–0.8 wt %) and the slightly disordered silicate structure in alite, resulting in broadened ^{29}Si resonances ranging from –67 to –77 ppm,⁸ make the $^{29}\text{Si}\{^{19}\text{F}\}$ MAS NMR experiments highly challenging in the present study.

The ^{29}Si MAS NMR spectrum (Figure 1a) of the white Portland clinker (wPc) exhibits a narrow resonance at $\delta(^{29}\text{Si}) = -71.3$ ppm from belite superimposed on a much broader peak from the 18 different Si sites in the monoclinic M_{III} form⁹ of alite. A deconvolution of the ^{29}Si MAS NMR spectrum, reveals that the wPc contains 57.7 wt % alite and 28.1 wt % belite, using a refined approach for quantitative ^{29}Si NMR analysis of anhydrous Portland

cements.¹⁰ The ^{19}F MAS NMR spectra of the commercial wPc (0.04 wt % F) and the corresponding modified clinkers with a higher fluorine content (0.77 wt %) both display a somewhat broadened ^{19}F resonance at $\delta(^{19}\text{F}) = -114.9$ ppm (*fwhm* = 14.9 ppm, Figure 1c,d) which is shifted slightly toward a lower frequency relative to the ^{19}F resonance observed for CaF₂ ($\delta(^{19}\text{F}) = -105.9$ ppm, *fwhm* = 6.8 ppm). The observation of a single resonance shows that the F[–] anions are in a similar structural environment, while the chemical shift indicates that they are not involved in Si–F or Al–F bonds which generally exhibit chemical shifts at lower frequencies.¹¹ The $^{29}\text{Si}\{^{19}\text{F}\}$ cross-polarization (CP) MAS NMR spectrum of the modified wPc (Figure 1b) shows overlapping resonances with an overall line shape that closely resembles the ^{29}Si NMR spectrum of the monoclinic M_{III} form for alite,⁸ thereby demonstrating that the fluoride ions are incorporated in the alite phase only.

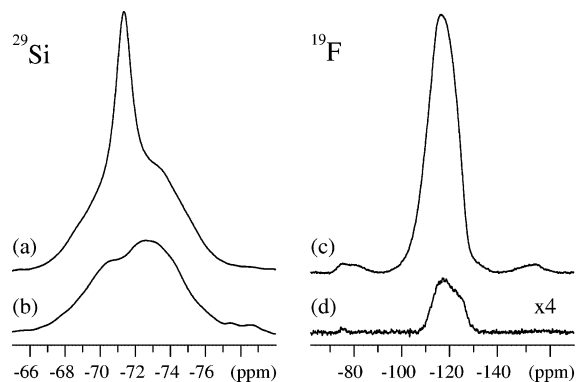


Figure 1. (a) ^{29}Si MAS and (b) $^{29}\text{Si}\{^{19}\text{F}\}$ CP/MAS NMR spectra (7.1 T) of the white Portland clinker (wPc) containing 0.77 wt % F, obtained with spinning speeds of $\nu_R = 7.0$ kHz and $\nu_R = 3.0$ kHz, respectively, and a CP contact time of 2.0 ms in part (b). Spin-echo ^{19}F MAS NMR spectra (7.1 T, $\nu_R = 12.0$ kHz) of (c) the modified Portland clinker (0.77 wt % F) and (d) the original wPc (0.04 wt % F).

Furthermore, $^{29}\text{Si}\{^{19}\text{F}\}$ CP/MAS NMR spectra of five modified wPc samples including 0.2–0.8 wt % F (Figure S1) show that the intensity of the alite resonance increases with increasing fluorine content. ^{27}Al MAS NMR spectra (14.1 T) of the same samples (Figure S2) demonstrate an increased incorporation of Al³⁺ guest ions in alite¹² when the fluorine content is increased. This strongly suggests that the substitution of oxygen by fluorine in alite is accompanied by a replacement of Si⁴⁺ by Al³⁺, in agreement with the earlier proposed Si⁴⁺ + O^{2–} → Al³⁺ + F[–] coupled substitution mechanism from selective fluoride dissolution measurements.⁵

Further insight into the location of the F[–] anions in alite is achieved from $^{29}\text{Si}\{^{19}\text{F}\}$ CP rotational-echo double resonance (REDOR)¹³ MAS NMR experiments (Figure 2). For the wPc with 0.77 wt % F, the difference in signal intensity ($\Delta S = S_0 - S$) between the ^{29}Si spin-echo (S_0) and the ^{19}F dephased REDOR

[†] Aarhus University.
[‡] Aalborg Portland A/S.

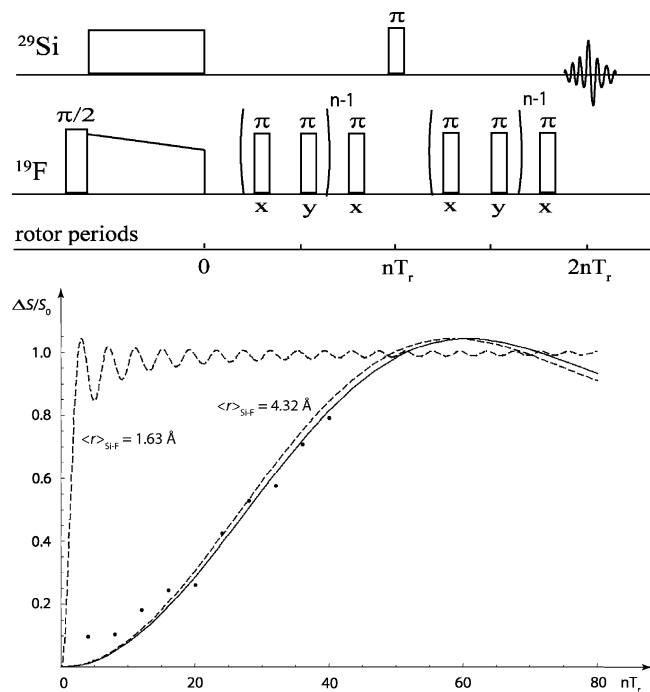


Figure 2. Results for the wPc containing 0.77 wt.% F, obtained with the CP-REDOR pulse sequence shown above the graph (7.1 T, $\nu_R = 10.0$ kHz, $T_r = 1/\nu_R = 0.1$ ms, 3.0 ms CP contact time). (●) Experimental REDOR fractions ($\Delta S/S_0$) and the result of numerical fitting of these data (solid line). Simulations are also shown for $r_{\text{Si-F}} = 1.63$ Å and $r_{\text{Si-F}} = 4.32$ Å (dashed lines), i.e., Si–F distances that match the mean Si–O bond length and the mean distance from the interstitial oxygens to their nearest Si atoms in the M_{III} form of alite, respectively. The fitting of the REDOR curves employed the simulation procedure described in ref 14 with the infinite sum of Bessel functions (J_k) truncated at $k = 10$.

spectra (S) results in the REDOR fractions ($\Delta S/S_0$) shown as a function of the dephasing time. These data are obtained for an optimized CP contact time of 3.0 ms (Figure S3); however, selected REDOR experiments for CP contact times of 1.0 and 7.0 ms give similar $\Delta S/S_0$ fractions which are expected to be within the error limits of the data in Figure 2. This independence of $\Delta S/S_0$ on CP contact time indicates a quite uniform distribution of fluoride ions in the alite lattice. This observation and the low fluorine content of the sample along with the low natural abundance for ^{29}Si (4.7%) implies that the REDOR fractions can be analyzed using the expression for the dipolar dephasing of an isolated ^{29}Si – ^{19}F spin pair. This approach¹⁴ results in a ^{29}Si – ^{19}F dipolar coupling constant of $d = \gamma_I \gamma_S \hbar \mu_0 / (8\pi^2 r^3) = 285$ Hz, corresponding to a ^{29}Si – ^{19}F distance of 4.29 Å.

The alite structure includes two different types of oxygen atoms, corresponding to the covalently bonded oxygens of the SiO_4 units and the “interstitial” oxygen sites which are not involved in Si–O bonds. Examination of the triclinic¹⁵ and monoclinic M_{III} ⁹ forms of alite reveals an average Si–O distance of 1.63 Å for the covalent Si–O bonds in both structures, while average internuclear distances of 4.28 Å and 4.32 Å are calculated for the interstitial oxygens and their nearest Si sites in the two forms, respectively. The REDOR curves for Si–F distances that equal the average Si–O length and the average distance from the interstitial oxygens to their nearest Si atoms are quite different (Figure 2). Furthermore, it is clearly observed that the experimental REDOR curve is very similar to the calculated curve for the F^- ions in the interstitial oxygen sites, demonstrating that the fluoride ions have a strong site preference for the interstitial oxygen sites of the alite structure for which one oxygen per formula unit (Ca_3SiO_5) is an interstitial oxygen. This

observation also explains the lack of incorporation of F^- ions in belite (Figure 1a,b), since β - Ca_2SiO_4 only includes oxygens in Si–O bonds.¹⁶

Assuming the F^- ions in alite are charge-balanced by only Al^{3+} ions in the tetrahedral sites results in the formula unit $\text{Ca}_{27}\text{Si}_{9-x}\text{Al}_x(\text{O}_b)_36(\text{O}_i)_{9-x}(\text{F}_i)_x$ where O_b and O_i denote the bonded and interstitial oxygens, respectively. This implies that the mineralizing effect of the fluoride ions associated with the entropy of mixing is limited by the fact that only one-fifth of the oxygen atoms are available for substitution by fluoride ions. The coupled incorporation of Al^{3+} ions in alite also contributes to the entropy of mixing; however, this effect is limited if the Al^{3+} ions are not randomly distributed over the tetrahedral sites but tend to order in the nearest vicinity of fluoride ions. Furthermore, other ions or the formation of vacancies may also contribute to the charge balance of the fluoride ions in alite. Consideration of the F^- guest ions only results in a maximum entropy of mixing for $x = 4.5$ in the formula unit given above, corresponding roughly to a quantity of 4.1 wt % F in pure alite and to 2.4 wt % F in the wPc containing 57.7 wt % alite. Of course, this solid solution is unlikely to be ideal, even at the high temperatures involved, and the enthalpy of mixing will limit the solubility of F in the alite phase to a lower concentration than this due to distortion of the structure from both fluorine and aluminum on the tetrahedral sites.

In conclusion, the present study has demonstrated that fluoride guest ions are only incorporated in the alite phase of a white Portland cement and with a clear site preference for the interstitial oxygen sites not involved in covalent Si–O bonds. This result may have an important impact on the optimization of the fluoride mineralization of Portland cements with the purpose of reducing the upper kiln temperature, by increasing the entropy of mixing, and thereby the energy consumption and CO_2 emission associated with Portland cement production.

Acknowledgment. The use of the facilities at the Instrument Centre for Solid-State NMR Spectroscopy, Aarhus University, sponsored by the Danish Natural Science Research Council is acknowledged. We thank the Danish National Advanced Technology Foundation for financial support.

Supporting Information Available: Sample preparation, experimental details, and additional NMR spectra. This material is available free of charge via the Internet at <http://pubs.acs.org>.

References

- (1) U.S. Department of the Interior, U.S. Geological Survey, *Mineral Commodity Summaries 2009*, United States Government Printing Office, Washington DC, U.S.A., 2009.
- (2) Damtoft, J. S.; Lukasik, J.; Herfort, D.; Sorrentino, D.; Gartner, E. M. *Cem. Concr. Res.* **2008**, *38*, 115.
- (3) Odler, I.; Abdul-Maula, S. *J. Am. Ceram. Soc.* **1980**, *63*, 654.
- (4) Shame, E. G.; Glasser, F. P. *Br. Ceram. Trans. J.* **1987**, *86*, 13.
- (5) Moir, G. K. *Phil. Trans. R. Soc. London, Ser. A* **1983**, *310*, 127.
- (6) Johansen, V.; Bhatti, J. I. In *Innovations in Portland cement manufacturing*; Bhatti, J. I., Miller, F. M., Kosmatka, S. H., Eds; Portland Cement Association: Skokie, IL, 2004; pp 369–402.
- (7) Fyfe, C. A.; Brouwers, D. H.; Lewis, A. R.; Chézeau, J.-M. *J. Am. Chem. Soc.* **2001**, *123*, 6882.
- (8) Skibsted, J.; Jakobsen, H. J.; Hall, C. *J. Chem. Soc., Faraday Trans.* **1995**, *91*, 4423.
- (9) Nishi, F.; Takeuchi, Y.; Maki, I. *Z. Kristallogr.* **1985**, *172*, 297.
- (10) Poulsen, S. L.; Kocaba, V.; Le Saout, G.; Jakobsen, H. J.; Scrivener, K. L.; Skibsted, J. *Solid State Nucl. Magn. Reson.* **2009**, *36*, 32.
- (11) (a) Liu, Y.; Tossell, J. *J. Phys. Chem. B* **2003**, *107*, 11280. (b) Youngman, R. E.; Sen, S. *J. Non-Cryst. Solids* **2004**, *349*, 10.
- (12) Skibsted, J.; Jakobsen, H. J.; Hall, C. *J. Chem. Soc., Faraday Trans.* **1994**, *90*, 2095.
- (13) Gullion, T.; Schaefer, J. *J. Magn. Reson.* **1989**, *81*, 196.
- (14) Mueller, K. T. *J. Magn. Reson., Ser. A* **1995**, *113*, 81.
- (15) Golovastikov, N. I.; Matveeva, R. G.; Belov, N. V. *Kristallografiya* **1975**, *20*, 721.
- (16) Jost, K. H.; Zeimer, B.; Seydel, R. *Acta Crystallogr.* **1977**, *B33*, 1696.

JA905223D